Active Vibration Suppression of Smart Cantilever Beam with Sliding Mode Observer Using Two Piezoelectric Patches

Shibly A. AL-Samarraie*   Mohsin N. Hamzah**
Imad A. Abdulsahib***

Department of Control and Systems Engineering / University of Technology
,*Department of Mechanical Engineering / University of Technology*
*Email: 60132@uotechnology.edu.iq
**Email: dr.mohsin@uotechnology.edu.iq
***Email: emad099@yahoo.com

Abstract

This paper presents a vibration suppression control design of cantilever beam using two piezoelectric patches. One patch was used as an actuator element, while the other was used as a sensor. The controller design was designed via the balance realization reduction method to elect the reduced order model that is most controllable and observable. the sliding mode observer was designed to estimate six states from the reduced order model but three states are only used in the control law. Estimating a number of states larger than that used is in order to increase the estimation accuracy. Moreover, the state estimation error is proved bounded. An optimal LQR controller is designed then using the estimated states with the sliding mode observer, to suppress the vibration of a smart cantilever beam via the piezoelectric elements. The control spillover problem was avoided, by deriving an avoidance condition, to ensure the asymptotic stability for the proposed vibration control design. The numerical simulations were achieved to test the vibration attenuation ability of the proposed optimal control. For 15 mm initial tip displacement, the piezoelectric actuator found able to reduce the tip displacement to about 0.1 mm after 4s, while it was 1.5 mm in the open loop case. The current experimental results showed a good performance of the proposed LQR control law and the sliding mode observer, as well a good agreement with theoretical results.

Keywords: Smart materials, Active vibration, Piezoelectric, Sliding mode observer, Model reduction, LQR controller.

1. Introduction

Active vibration control is a technique that is used for suppression structural vibrations, using this technique to smart structures becomes of great interest and getting much more important. One way of making the structure a smart one is performed by the use of piezoelectric materials, which can be used as sensors and actuators. They are flexible enough to be placed in a variety of places and have the capacity to work in wide ranges of frequencies [1]. Piezoelectric materials have simple mechanical properties, small volume, light weight, and good ability to perform vibration

control [2]. One of the application of piezoelectric smart structures is the control and suppression of unwanted structural vibrations [3]. In these materials electricity is produced by pressure, called direct effect. Conversely, subjecting these materials to an electric field produces a deformation, converse effect. The piezoelectric sensor senses the external disturbances and generates voltage due to the direct effect, while piezoelectric actuator produces force, due to the converse effect, that can be used as a controlling force [4].

Modelling continuous mechanical structures subjected to dynamic loadings is not an easy task.

Scarce analytical solutions for specific situations are available. The discretization of these structures is an alternative and basic step for further analysis. The finite element methods (FEM) is an efficient tool for this purpose [5].

In the finite element modeling, the structure is modeled to retain large number of degrees of freedoms. In active vibration control, the use of smaller order model has computational advantages. Therefore, it is essential to apply model reduction techniques for getting a reduced model for designing the control law. One of these techniques is based on balance realization method [6]. The approach taken for reduction the order of a given model based on removal the coordinates, that are the least controllable and observable. To implement this idea, a measure of the degree of controllability and observability is required [7]. For closed-loop system, it is not always possible to get a control law that cause eigenvalues to have the required and desired values. The system is completely controllable if every state variable can be affected in such a way as to cause it to reach a particular value within a finite amount of time by some unbounded control [6]. However, an alternative, more useful measure is provided for asymptotically stable systems of the form given by equations by defining the controllability gramian. Gramian matrices can be used for checking if a system is controllable and observable [6].

The control of the vibration of a smart structure is usually performed via a controller that based on the reduced order model (ROM). Once a ROM based controller is applied to the full order system, actuator forces will reduce the vibration of the lower modes. However, this will also influence the residual modes of the structure, producing undesirable vibration due to the un-modeled dynamics. This phenomenon is known as control spillover [9]. Similarly, the sensor will sense the deflection from the lower modes as well as from the other modes, this is known as observation spillover. Spillover effects are undesirable and may cause performance degradation and even system instability [10]. Indeed, one way to avoid a spillover, which comes from the state estimation or observation process, is to use an observer for estimating the states with minimal error.

Numerous control strategies have been suggested to suppress the vibration of flexible structures for the flexible systems. Some of these studies are state feedback control, linear quadratic regulator (LQR) approach [11], H_2 control, H_∞ control [12] and sliding mode control [13]. The

theory of optimal control is concerned with operating a dynamic system at minimum cost. The case, where the system dynamics are described by a set of linear differential equations and the cost is described by a quadratic function, is called the LQR problem. The settings of a regulating controller governing a controlled system are found by using a mathematical algorithm that minimizes a cost function with weighting factors. The cost function is a sum of the deviations of key measurements from their desired values. Often the magnitude of the control action itself is included in this sum so as to bound the energy spent by the control action [11]. The LQR is the most commonly used controller in smart structures [14-17].

State measurement is required for the controller; an observer is usually designed to estimate the states. Observers are dynamic systems that can be used to estimate the unavailable state variables of a plant. Luenberger observer [18], used a dynamical linear system to generate estimates of the plant states. In some cases, some of the inputs to the system are unknown. This led to the development of the unknown input observer. For the smart beam, which modeled by FEM with a reduced number of states, the remaining states which are acting on the reduced model can be regarded as unknown inputs.

Sliding mode theory is a robust control approach in treating disturbances and modeling uncertainties through the concepts of sliding surface design and equivalent control [13]. Based on the equivalent control, the sliding mode control theory can be used as an observer to estimate the system states. The sliding mode observer (SMO) are able to ensure finite-time convergence of the output estimation error even in the presence of the unknown inputs. Additionally, they can be used to reconstruct unknown inputs using equivalent control methods [19]. The method V-function, [20], has been used to formulate sliding mode observers design which lead the state estimation errors approach to zero asymptotically with matched uncertainties. The main advantage of using sliding-mode observers is that, while in sliding, they are insensitive to the matched unknown inputs. Moreover, they can be used to reconstruct unknown inputs, which could be a combination of system disturbances [21]. Many researchers were interested in designing sliding mode observers for uncertain dynamical systems; such as Utkin et al. [22], Walcot et al. [23], Zak et al. [24], Edwards et al. [19], and Slotine et al. [25].

This paper focuses on designing an optimal LQR controller by using sliding mode observer to attenuate the vibration of a smart cantilever beam. Piezoelectric elements are used as an actuator and a sensor. The utilized model for control design purpose is the reduced order model that is obtained according to the balance realization method. Based on the equivalent control, the SMO is designed with estimation error related to the ROM. To avoid control spillover, an avoidance condition, using complete system dynamics, was derived.

2.   Modeling of Smart Cantilever Beam

Figure (1) depicting the smart cantilever beam considered in this work. The beam is bonded with a pair of piezoelectric patches, working as a sensor and an actuator, at the indicated position. The piezoelectric material used in this work is the Lead-Zirconate-Titanate (PZT). Using Euler-Bernoulli beam equation, the partial differential equation of the beam can be written as [26];

$$c^2 \frac{\partial^4 w(x,t)}{\partial x^4} + \frac{\partial^2 w(x,t)}{\partial t^2} = 0 \qquad \ldots(1)$$

where $c^2 = EI/\rho A$, $w(x,t)$ is the deflection along the x-axis, E is the Young's modulus, I is the moment of inertia, A is the cross sectional area, and ρ is the density. Equation (1) can be solved by using the assumed mode approach, which yields finite dimensional ordinary differential equation set.
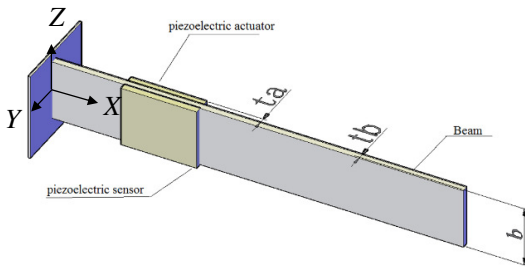

Fig. 1. Flexible smart cantilever beam.

The dynamic equation of the smart structure is obtained by using both regular beam element and piezoelectric beam elements. The mass and stiffness matrices of the smart structure include the mass and stiffness of the sensor/actuator [27]. The smart beam, shown in Figure (1), is modelled in state space form using the FEM, the beam is divided into six equal finite elements. The sensor

and actuator were integrated on the top and bottom surfaces at the second element from the fixed end of the beam.

A beam element is considered with two nodes at its end. Each node is considered to have two degrees of freedom (DOF), i.e. translation (in y-direction) and rotation. The mass and stiffness matrix are derived using shape functions for the beam element. The inertia force appears in the governing differential equation of the beam, Equation (1), involves a fourth order derivative w.r.t. x, and a second order derivative w.r.t. time (acceleration). The solution of this equation is assumed as a cubic polynomial function [28].

$$w(x) = a_1 + a_2\, x + a_3\, x^2 + a_4\, x^3 \qquad \ldots(2)$$

where $w(x)$ is displacement function which satisfies the fourth order partial differential equation, here x is the local coordinate of the element. The constants a_1 to a_4 be obtained by using the boundary conditions at both the nodal points (fixed end and free end). And it can be represented in a matrix form as, [29]

$$\begin{bmatrix} w_1 \\ \theta_1 \\ w_2 \\ \theta_2 \end{bmatrix} = \begin{bmatrix} 1 & 0 & 0 & 0 \\ 0 & 1 & 0 & 0 \\ 1 & l & l^2 & l^3 \\ 0 & 1 & 2l & 3l^2 \end{bmatrix} \begin{bmatrix} a_1 \\ a_2 \\ a_3 \\ a_4 \end{bmatrix} \qquad \ldots(4)$$

where $w_1, \theta_1, w_2,$ and θ_2 are the degree of freedom at node 1 and 2, respectively, and l is the length of the element.

Accordingly, the mass matrix is given as, [29]

$$M_b = \rho_b A_b \int_{l_b} N N^T dx =$$
$$\frac{\rho_b A_b l_b}{420} \begin{bmatrix} 156 & 22l_b & 54 & -13l_b \\ 22l_b & 4l_b^2 & 13l_b & -3l_b^2 \\ 54 & 13l_b & 156 & -22l_b \\ -13l_b & -3l_b^2 & -22l_b & 4l_b^2 \end{bmatrix} \qquad \ldots(4)$$

where M_b is the mass matrix of regular beam, N is the shape function. Also for the strain energy the stiffeness matrix is given by [29]:

$$K_b = E_b I_b \int_{l_b} N_2 N_2^T\, dx =$$
$$\frac{E_b I_b}{l^3} \begin{bmatrix} 12 & 6l & -12 & 6l \\ 6l & 4l^2 & -6l & 2l^2 \\ -12 & -6l & 12 & -6l \\ 6l & 2l^2 & -6l & 4l^2 \end{bmatrix} \qquad \ldots(5)$$

where K_b is the stiffeness matrix of regular beam,
Eventually the equation of motion according to the Lagrangian equation is [30]:

$$M_b \, \ddot{q} + K_b q = f_b \qquad \qquad \ldots(6)$$

or

$$\frac{\rho_b A_b}{420} \begin{bmatrix} 156 & 22l_b & 54 & -13l_b \\ 22l_b & 4l_b^2 & 13l_b & -3l_b^2 \\ 54 & 13l_b & 156 & -22l_b \\ -13l_b & -3l_b^2 & -22l_b & 4l_b^2 \end{bmatrix} \begin{bmatrix} \ddot{w}_1 \\ \ddot{\theta}_1 \\ \ddot{w}_2 \\ \ddot{\theta}_2 \end{bmatrix} +$$

$$\frac{E_b I_b}{l^3} \begin{bmatrix} 12 & 6l_b & -12 & 6l_b \\ 6l_b & 4l_b^2 & -6l_b & 2l_b^2 \\ -12 & -6l_b & 12 & -6l_b \\ 6l_b & 2l_b^2 & -6l_b & 4l_b^2 \end{bmatrix} \begin{bmatrix} w_1 \\ \theta_1 \\ w_2 \\ \theta_2 \end{bmatrix} = \begin{bmatrix} F_1 \\ M_1 \\ F_2 \\ M_2 \end{bmatrix}$$

$$\ldots(7)$$

where F_1, F_2, M_1, M_2 are the forces and the bending moments acting on nodes 1 and 2 respectively Figure (1). When PZT patches are assumed as Euler-Bernoulli beam elements the elemental mass and stiffness matrices of PZT beam element can be computed in similar fashion as [31]:

$$M_p = \frac{\rho_p A_p l_p}{420} \begin{bmatrix} 156 & 22l_p & 54 & -13l_p \\ 22l_p & 4l_p^2 & 13l_p & -3l_p^2 \\ 54 & 13l_p & 156 & -22l_p \\ -13l_p & -3l_p^2 & -22l_p & 4l_p^2 \end{bmatrix}$$

$$\ldots(8)$$

$$K_p = \frac{E_p I_p}{l^3} \begin{bmatrix} 12 & 6l_p & -12 & 6l_p \\ 6l_p & 4l_p^2 & -6l_p & 2l_p^2 \\ -12 & -6l_p & 12 & -6l_p \\ 6l_p & 2l_p^2 & -6l_p & 4l_p^2 \end{bmatrix} \qquad \ldots(9)$$

In which $EI = E_b I_b + 2E_p I_p$ is the flexural rigidity and $\rho A = b(\rho_b t_b + 2\rho_p t_p)$ is the mass per unit length, t_p is the thickness of PZT patches, and $I_p = \frac{b \, t_a^3}{12} + bt_a \left(\frac{t_a+t_b}{2}\right)^2$. So the element mass and stiffness matrices are:

$$M_e = \frac{\rho A l_b}{420} \begin{bmatrix} 156 & 22l_b & 54 & -13l_b \\ 22l_b & 4l_b^2 & 13l_b & -3l_b^2 \\ 54 & 13l_b & 156 & -22l_b \\ -13l_b & -3l_b^2 & -22l_b & 4l_b^2 \end{bmatrix}$$

$$\ldots(10)$$

$$K_e = \frac{E I}{l_p^3} \begin{bmatrix} 12 & 6l_b & -12 & 6l_b \\ 6l_b & 4l_b^2 & -6l_p & 2l_b^2 \\ -12 & -6l_b & 12 & -6l_b \\ 6l_b & 2l_b^2 & -6l_b & 4l_b^2 \end{bmatrix} \qquad \ldots(11)$$

2.1. Sensor and Actuator Equations

The sensor equation is derived from the direct piezoelectric equation, which is used to calculate the total charge created by the strain in the structure. The output charge can be transformed into the sensor current $i(t)$ [32]:

$$i\,(t) = z \, e_{31} \, b \int_{x_i}^{x_i+l_b} N_2{}^T \dot{q} \, dx \qquad \ldots(12)$$

where, $z = \frac{t_b}{2} + t_a$ and N_2 is the second spatial derivative of the shape function, e_{31} is the piezoelectric stress constant.

The output current of the piezoelectric sensor measures the moment rate of the flexible beam. This current is converted into the open circuit sensor voltage $V_s(t)$ using a signal-conditioning device with the gain G_c. Thus [30]:

$$V_s(t) = \begin{bmatrix} 0 & -G_c z \, e_{31} \, b & 0 & G_c \, z \, e_{31} \, b \end{bmatrix} \begin{bmatrix} \dot{w}_1 \\ \dot{\theta}_1 \\ \dot{w}_2 \\ \dot{\theta}_2 \end{bmatrix}$$

$$= Sc \begin{bmatrix} 0 & -1 & 0 & 1 \end{bmatrix} \begin{bmatrix} \dot{w}_1 \\ \dot{\theta}_1 \\ \dot{w}_2 \\ \dot{\theta}_2 \end{bmatrix} = p^T \dot{q} \qquad \ldots(13)$$

where $S_c = G_c \, z \, e_{31} \, b$ and p is a constant vector depends on the type of sensor, its characteristics and its location on the beam.

The actuator equation is derived from the converse piezoelectric equation. The strain developed ϵ_x by the electric field E_f on the actuator layer is given by [33]:

$$\epsilon = dE_f \qquad \qquad \ldots(14)$$

where, $E_f = \frac{V_a(t)}{t_a}$ is the electric field, and $V_a(t)$ is the input voltage applied to the piezoelectric actuator in the thickness direction t_a. Then the stress σ_a that developed by the actuator is given by: [34]

$$\sigma_a = E_p \, d_{31} \left(\frac{V_a(t)}{t_a}\right) \qquad \ldots(15)$$

where E_p is the Young's modulus of the piezoelectric and d_{31} is piezoelectric strain constant.

The bending moment of the piezoelectric element is given by:

$$dM_a = E_p \, I_p \, \frac{d^2w}{dx^2} \qquad \qquad \ldots(16)$$

The resultant moment M_a acting on the beam element due to the applied voltage V_a is determined by integrating the stress in Equation (15) throughout the structure thickness as:

$$M_a = E_p \, d_{31} z \, V_a(t) \qquad \ldots(17)$$

The control force f_{ctrl} produced by the actuator that is applied on the beam element is obtained as [30]:

$$f_{ctrl} = E_p d_{31} b \, z \, [\, -1 \; 0 \; 1 \; 0\,]^T \, V_a(t) \qquad \ldots(18)$$

Alternatively, f_{ctrl} can be expressed as:

$$f_{ctrl} = h \, V_a\,(t) \qquad \ldots(19)$$

$$h = E_p \, d_{31} \, b \, z \, [\, -1 \; 0 \; 1 \; 0\,]^{\mathrm{T}} \qquad \ldots(20)$$

3. Dynamic Equation of Smart Structure

The element mass and stiffness matrices, Equation (10) and Equation (11), can be assembled using the standard FEM procedure, to obtain the global mass and stiffness matrices of the entire beam. The beam is divided into six finite elements with two piezo-patches placed at the specified location. The equation of motion of the smart structure is given by [28]:

$$M\,\ddot{q} + Kq = f_{ext} + f_{ctrl} = f \qquad \ldots(21)$$

where M, K, f_{ext}, f_{ctrl} and f are the global mass matrix, stiffness matrix, external force vator, the controlling force vector (from the actuator), and the total force coefficient vector, respectively.

The generalized structural modal damping matrix D is introduced into Equation (21) by using[35, 36]:

$$D = \alpha M + \beta K \qquad \ldots(22)$$

where α and β are the frictional damping constant and the structural damping constant respectively. When applying the cantilever beam boundary condition, the system equation of motion for the six element cantilever beam is:

$$M\,\ddot{q} + D\dot{q} + Kq = f \qquad \ldots(23)$$

For free vibration condition f_{ext} equal to zero, so the remaining applied force on the system is the controlling force f_{ctrl} exerted by the controller.

3.1 State Space Model of the Smart Beam

Model reduction in modern control theory needs a state space form for the mathematical model of a plant. Consequently, the mathematical model of smart flexible cantilever beam can be written in state space form as follows [37]; let

$$q = \begin{bmatrix} q_1 \\ q_2 \end{bmatrix} = \begin{bmatrix} x_1 \\ x_2 \end{bmatrix} = x \;, \quad \dot{q} = \begin{bmatrix} \dot{q}_1 \\ \dot{q}_2 \end{bmatrix} = \begin{bmatrix} \dot{x}_1 \\ \dot{x}_2 \end{bmatrix} = \begin{bmatrix} x_3 \\ x_4 \end{bmatrix}, \quad \text{and}$$

$$\ddot{q} = \begin{bmatrix} \dot{x}_3 \\ \dot{x}_4 \end{bmatrix},$$

then the smart cantilever beam state space model is;

$$M \begin{bmatrix} \dot{x}_3 \\ \dot{x}_4 \end{bmatrix} + D \begin{bmatrix} x_3 \\ x_4 \end{bmatrix} + K \begin{bmatrix} x_1 \\ x_2 \end{bmatrix} = f_{ctrl} \qquad \ldots(24)$$

which yields to

$$\begin{bmatrix} \dot{x}_1 \\ \dot{x}_2 \\ \dot{x}_3 \\ \dot{x}_4 \end{bmatrix} = \begin{bmatrix} 0 & I \\ -M^{-1}K & -M^{-1}D \end{bmatrix} \begin{bmatrix} x_1 \\ x_2 \\ x_3 \\ x_4 \end{bmatrix} +$$
$$\begin{bmatrix} 0 \\ M^{-1}h \end{bmatrix} u(t) \qquad \ldots(25)$$

And in a matrix form

$$\dot{x} = Ax(t) + Bu(t) \qquad \ldots(26)$$

where $x = \begin{bmatrix} x_1 \\ x_2 \\ x_3 \\ x_4 \end{bmatrix}, A = \begin{bmatrix} 0 & I \\ -M^{-1}K & -M^{-1}D \end{bmatrix}$,

$B = \begin{bmatrix} 0 \\ M^{-1}h \end{bmatrix}$ and $u(t) = V_a(t)$.

with appropriate zero and identity matrices dimensions. The sensor voltage is taken as the output of the system and the output equation is obtained as:

$$y(t) = V_s(t) = p^T \dot{q} = p^T \begin{bmatrix} x_3 \\ x_4 \end{bmatrix} \qquad \ldots(27)$$

Thus, the sensor output equation in state space form is given by:

$$y(t) = [0 \quad p^T] \begin{bmatrix} x_1 \\ x_2 \\ x_3 \\ x_4 \end{bmatrix} \text{ or, } y(t) = Cx(t) \qquad \ldots(28)$$

where $C = [0 \quad p^T]$. Eventually, the single input single output state space model of the smart beam is given by Equations (26) and (28):

$$\left. \begin{array}{l} \dot{x} = Ax\,(t) + Bu(t) \\ y = Cx(t) \end{array} \right\} \qquad \ldots(29)$$

with

$$A = \begin{bmatrix} 0 & I \\ -M^{-1}K & -M^{-1}D \end{bmatrix}_{24*24}$$
$$B = \begin{bmatrix} 0 \\ M^{-1}h \end{bmatrix}_{24*1} \qquad \Bigg\} \qquad ...(30)$$
$$C = [0 \quad p^T]_{1*24}$$

3.2. Model Reduction

Using the FEM the structure is modeled to retain large (but finite) number of DOF. In active vibration control, the use of smaller order model has computational advantages. Therefore, it is necessary to apply a model reduction technique to the state space representation [6]. In this work the 24th order system model, obtained from the FEM modelling, is reduced to the three order using a model reduction technique based on balance realization.

In this approach the state coordinate basis is selected such that the controllability and observability grammians are diagonal matrix and equal, normally with the diagonal entries of σ in descending order the state space representation is then called balanced realization [6].

To implement this idea, a measure of the degree of controllability and observability is needed. However, an alternative, more useful measure is provided for asymptotically stable systems of the form given by equations by defining the controllability grammian, denoted by W_C, as [6]:

$$W_C^2 = \int_0^\infty e^{At} BB^T e^{A^T t} dt \qquad ...(31)$$

And the observability grammian, denoted by W_O, as [6]:

$$W_O^2 = \int_0^\infty e^{A^T t} C^T C e^{At} dt \qquad ...(32)$$

where the matrices A, B, and C are defined in Equation (30). The properties of these matrices provide useful information about the controllability and observability of the closed-loop system. If the system is controllable (or observable), the matrix W_C (or W_O) is nonsingular [38]. These grammians characterize the degree of controllability and observability by quantifying just how far away from being singular the matrices W_C and W_O are [6].

Applying the idea of singular values as a measure of rank deficiency to the controllability and observability grammians yields a systematic model reduction method. The matrices W_C and W_O are real and symmetric and hence are similar

to a diagonal matrix. There is equivalent system for which these two grammians are both equal and diagonal. Such a system is called balanced system, and W_C and W_O must satisfy the following two Liapunov-type equations: [39]

$$A W_C^2 + W_C^2 A^T = -BB^T \\ A^T W_O^2 + W_O^2 A = -C^T C \Bigg\} \qquad ...(33)$$

Now to transform the system to a balance realization form, the determination of a transformation matrix P_G that will transform the system in Equation (29) to:

$$\dot{x}' = A'x' + B'u \\ y = C'x' + Du \Bigg\} \qquad ...(34)$$

is required, where $A' = P_G^{-1}AP_G$, $B' = P_G^{-1}B$ and $C' = CP_G$. The controllability and observability grammians matrices are diagonal and equal

$$\widehat{W}_C = \widehat{W}_O = \Sigma = diag(\sigma_1, \sigma_2, \dots \dots, \sigma_n)$$

where $\widehat{W}_C$ and $\widehat{W}_O$ are the controllability and observability grammians for system after applying the transformation P and the numbers σ_i are the singular values of the grammians and are ordered such that $\sigma_i > \sigma_{i+1}$, $i = 1,2, \dots, n$

Therefore, the pair (A', B') could be uncontrollable pair since some of σ_j could be equal to zero. Indeed, there exist a subsystem, i.e. a reduced order model, which is still controllable and observable.

Choosing the matrix P_G in the form

$$P_G = G^{-1}U\Sigma^{\frac{1}{2}} \qquad ...(35)$$

the grammians W_c^2 and W_O^2 will transformed to become equal and transform the system in Equation (29) to a balanced realization form. Namely,
$$\widehat{W}_C = \widehat{W}_o = \Sigma \qquad ...(36)$$

where Σ can be written in terms of two set of the singular values $\sigma_{(1)}$ and $\sigma_{(2)}$ as

$$\Sigma = \begin{bmatrix} \sigma_{(1)} & 0 \\ 0 & \sigma_{(2)} \end{bmatrix} \qquad ...(37)$$

In this representation $\sigma_{(1)}$ describes the "strong" sub-systems to be retained and $\sigma_{(2)}$ the "weak" sub-systems to be deleted. Conformally partitioning the matrices as

$$A' = \begin{bmatrix} A_{11} & A_{12} \\ A_{21} & A_{22} \end{bmatrix}$$
$$B' = \begin{bmatrix} B_1 \\ B_2 \end{bmatrix} \qquad \qquad \text{...(38)}$$
$$C' = [C_1 \quad C_2]$$

and truncating the model, retaining $A_{1r} = A_{11}$, $B_r = B_1$ and $C_r = C_1$ as the reduced system, and deleting the "weak" internal subsystems [6].

4. LQR State Feedback Control Design

The LQR is an optimal control approach to determine control signals that will cause a process to satisfy some physical constraints, and at the same time (maximize or minimize) a chosen performance index or cost function [11]. To design an LQR control, to the reduced order model of the smart beam, the Reduced Model (RM) and the Residual Model (RSM) [9] are presented here as follows; according to the balance realization the linear state model for the cantilever beam, as given in Equation (34) are rewritten as follow; [29]

$$\begin{rcases} \dot{x}_r = A_{1r}x_r + A_{1R}x_R + B_1u \\ \dot{x}_R = A_{2r}x_r + A_{2R}x_R + B_2u \\ y = C_r x_r + C_R x_R \end{rcases} \qquad \text{...(39)}$$

where $x_r \in \mathcal{R}^r$, is the reduced model states, $x_R \in \mathcal{R}^{n-r}$ is the residual model states, and

$$A = \begin{bmatrix} A_{1r}^{r \times r} & A_{1R}^{r \times (n-r)} \\ A_{2r}^{(n-r) \times r} & A_{2R}^{(n-r) \times (n-r)} \end{bmatrix},$$

$$B = \begin{bmatrix} B_1^{r \times 1} \\ B_2^{(n-r) \times 1} \end{bmatrix},$$

$$C = [C_r^{1 \times r} \quad C_R^{1 \times (n-r)}]$$

The pair (A_{1r}, B_1) is the controllable pair and (A_{1r}, C_r) is the observable pair with highest controllability and observability grammian. From Equation (39), the reduced model of the transformed model, which given in Equation (34), is

$$\dot{x}_r = A_{1r}x_r + B_1u \qquad \qquad \text{...(40)}$$

Note that r represents also the number of the states that will be used in the control design.

In the second step the performance index J, is defined for the linear regulator problem as [6];

$$J = \frac{1}{2} \int_t^\infty (x_r^T Q \, x_r + u^T R \, u) \, dt, \qquad \text{...(41)}$$

where Q and R are symmetric positive definite weighting matrices. The larger the matrix Q, the more emphasis is placed by optimal control on returning the system to zero, since the value of x corresponding to the minimum of the quadratic form $x_r^T Q \, x_r$ is $x = 0$. On the other hand, increasing R has the effect of reducing the amount, or magnitude, of the control effort allowed [6].

The optiumal control law that will minimize J is given by [40].

$$u(t) = -R^{-1} B_1 P x(t) = -K(t)x(t) \qquad \text{...(42)}$$

where P is the solution to the algebraic Riccati Equation [15].

$$Q(t) - PB_1 R^{-1} B_1^T P + A_{1r}^T P + PA_{1r} = 0 \text{ ...(43)}$$

The linear controller, as in Equation (42), that grantted asymptotic stabilty of the reduce model, may also cause the instability for the system dynamic. This type of instability is named as the control spillover.

4.1 Control Spillover Problem and Avoidance Condition.

Spillover phenomenon occurs because that the unmodeled dynamics, which are not included in reduced order model, is excited by the control input as in the case of the reduced model. As a result the complete system model may have positive eigenvalue that leads to system instability. In order to avoid the control spillover, an avoidnace condition is derived as follows; let the matrix Δ be defined as;

$$\Delta = \begin{bmatrix} (A_{1r} - B_1K) & A_{1R} \\ (A_{2r} - B_2K) & A_{2R} \end{bmatrix} \qquad \text{...(44)}$$

which represents the whole model matrix after applying the proposed LQR control. In order to avoid control spillover the matrix Δ must be Hurwitz with its minimum absolute real eigenvalue is larger than theabsolute real eigenvalue of the matrix A Equation (29). Namely, if R_i^C represent the real term to eigenvalue of Δ and R_i^O represent the real term to eigenvalue of A then the avoidance condition is;

$$R^C = \min_{i=1 \to n} \left| R_i^C \right| > \min_{i=1 \to n} \left| R_i^O \right| = R^O$$

When difference between R^C and R^O is large, the vibration is attenuated effectively since the eigenvalue placed at R^O is the dominant one which shaped the cantilever beam response.

5. Sliding Mode Observer

For a large scale system, like the vibration control problem, the control spillover is not the only source for instability. There is another source of instability comes from imperfect or unprecise estimation for the states that are required for feeding back in the control law [13]. In fact the only way to avoid spillover that comes from the state estimation or observation process is to use an observer that estimates the states with minimal error. In the present work the Sliding Mode Observer (SMO) is used to estimate the states which it required in the control law Equation (42). The advantage of using SMO is to ensure that the difference between the system and observer outputs convergence to zero in a finite-time even in the presence of the unknown inputs. Additionally, the SMO can be used also to reconstruct unknown inputs using equivalent control method [21]. In the present work, the unknown input represents the residual term $(A_{1R}x_R)$ for the x_r dynamics Equation (39) and the corresponding reduced order model in Equation (40).

For the linear time invariant system; Equation (39)

$$\left.\begin{array}{l} \dot{x}_r = A_{1r}x_r + B_1 u + D\xi \\ y = C_r x_r \end{array}\right\} \qquad \text{...(45)}$$

where the unknown input $\xi = x_R \in \mathcal{R}^{n-r}$ and $D = A_{1R} \in \mathcal{R}^{r \times n-r}$. Now decompose x_r to $x_r = [x_1 \quad x_2]^T$ and C_r to $C_r = [C_1 \quad C_2]$, then the output y is:

$$y = C_r x_r = C_1 x_1 + C_2 x_2 \qquad \text{...(46)}$$

where $x_1 \in \mathcal{R}^{r-1}$, $x_2 \in \mathcal{R}^1$, $C_1 \in \mathcal{R}^{1 \times (r-1)}$ $C_2 \in \mathcal{R}^1$, where one of the attached piezoelectric patches is used as a sensor, and $\det(C_2) \neq 0$. Note that r represents the number of the estimated states which it selected later equal to six. Accordingly Equation (45), in terms of x_1 and x_2, can be written as

$$\left.\begin{array}{l} \dot{x}_1 = A_{11}x_1 + A_{12}x_2 + B_1 u + D_1 \xi \\ \dot{x}_2 = A_{21}x_1 + A_{22}x_2 + B_2 u + D_2 \xi \end{array}\right\} \qquad \text{...(47)}$$

where $B_1 \in \mathcal{R}^{(r-1) \times 1}$, $B_2 \in \mathcal{R}^1$, $D_1 \in \mathcal{R}^{(r-1) \times n-r}$ and $D_2 \in \mathcal{R}^{1 \times n-r}$. Equation (47) can be written in terms of x_1 and y as follows;

$$\left.\begin{array}{l} \dot{x}_1 = \tilde{A}_{11}x_1 + \tilde{A}_{12}y + \tilde{B}_1 u + \tilde{D}_1 \xi \\ \dot{y} = \tilde{A}_{21}x_1 + \tilde{A}_{22}y + \tilde{B}_2 u + \tilde{D}_2 \xi \end{array}\right\} \qquad \text{...(48)}$$

where x_2 is replaced by,

$$x_2 = C_2^{-1}(y - C_1 x_1) \qquad \text{...(49)}$$

and,

$$\tilde{A}_{11} = A_{11} - A_{12}C_2^{-1}C_1, \quad \tilde{A}_{12} = A_{12}C_2^{-1},$$
$$\tilde{A}_{21} = C_1 A_{11} + C_2 A_{21} - (C_1 A_{12} + C_2 A_{22})C_2^{-1}C_1$$
$$\tilde{A}_{22} = (C_1 A_{12} + C_2 A_{22})C_2^{-1}$$
$$\tilde{B}_1 = B_1, \quad \tilde{B}_2 = C_1 B_1 + C_2 B_2$$
$$\tilde{D}_1 = D_1,, \quad \tilde{D}_2 = C_1 D_1 + C_2 D_2,$$

Since $|C_2| \neq 0$, the transformation matrix between (x_1, x_2) and (x_1, y),

$$\begin{bmatrix} x_1 \\ y \end{bmatrix} = T_1 \begin{bmatrix} x_1 \\ x_2 \end{bmatrix} = \begin{bmatrix} I_{(r-1)} & O_{(r-1) \times 1} \\ C_1 & C_2 \end{bmatrix} \begin{bmatrix} x_1 \\ x_2 \end{bmatrix} \quad \text{...(50)}$$

is nonsingular.

To this end the proposed SMO to the system dynamic model, as given in Equation (48), is as follows;

$$\left.\begin{array}{l} \dot{\hat{x}}_1 = \tilde{A}_{11}\hat{x}_1 + \tilde{A}_{12}\hat{y} + \tilde{B}_1 u - Lv \\ \dot{\hat{y}} = \tilde{A}_{21}\hat{x}_1 + \tilde{A}_{22}\hat{y} + \tilde{B}_2 u - v \end{array}\right\} \qquad \text{...(51)}$$

The error dynamics between the observer Equation (51) and the system Equation (48) is governed by

$$\left.\begin{array}{l} \dot{e}_1 = \tilde{A}_{11}e_1 + \tilde{A}_{12}e_y - Lv - \tilde{D}_1 \xi \\ \dot{e}_y = \tilde{A}_{21}e_1 + \tilde{A}_{22}e_y - v - \tilde{D}_2 \xi \end{array}\right\} \qquad \text{...(52)}$$

where $e_1 = \hat{x}_1 - x_1$ and $e_y = \hat{y} - y$.

To examine the stability of the error dynamics, the equivalent control is utilized as follows; first the output error e_y is guaranteed to reach zero value in a finite time if v is selected as a discontinuous function of e_y

$$v = \tilde{A}_{22}e_y + \eta * sgn(e_y) \qquad \text{...(53)}$$

where $sgn(e_y)$ is the signum function defined as follows;

$$sgn(e_y) = \begin{cases} 1 \; if \; e_y > 0 \\ -1 \; if \; e_y < 0 \end{cases} \qquad …(54)$$

and η is the discontinuous gain that must satisfy the following condition

$$\eta > \left| \tilde{A}_{21}e_1 - \tilde{D}_2\xi \right| \qquad …(55)$$

If η satisfies the inequality (55), then the sliding motion will ocuure on the sliding surface $e_y = 0$ after a finite time. By taking the initial condition for observer design as;

$$(\hat{x}_1, \hat{y})_{t=0} = (0, y(0)) \qquad …(56)$$

and with v as in Equation (53), we have $e_y = 0, \dot{e}_y = 0$ from the first instant, i.e. $\forall t \geq 0$. The error dynamic stability based on the equivalent control is examined here as follows;

$$\begin{cases} \dot{e}_1 = \tilde{A}_{11}e_1 + \tilde{A}_{12}e_y - Lv - \tilde{D}_1\xi \\ \dot{e}_y = \tilde{A}_{21}e_1 + \tilde{A}_{22}e_y - v - \tilde{D}_2\xi \end{cases}_{eq} = $$

$$\begin{cases} \dot{e}_1 = \tilde{A}_{11}e_1 - Lv_{eq} - \tilde{D}_1\xi \\ 0 = \tilde{A}_{21}e_1 - v_{eq} - \tilde{D}_2\xi \end{cases},$$

which yields

$$\begin{cases} \dot{e}_1 = \tilde{A}_{11}e_1 + \tilde{A}_{12}e_y - Lv - \tilde{D}_1\xi \\ \dot{e}_y = \tilde{A}_{21}e_1 + \tilde{A}_{22}e_y - v - \tilde{D}_2\xi \end{cases}_{eq} = $$

$$\begin{cases} \dot{e}_1 = (\tilde{A}_{11} - L\tilde{A}_{21})e_1 + (L\tilde{D}_2 - \tilde{D}_1)\xi \\ v_{eq} = \tilde{A}_{21}e_1 - \tilde{D}_2\xi \end{cases} \quad …(57)$$

where v_{eq} is computed at $e_y = \dot{e}_y = 0$.

From Equation (57) the unknown input term $(L\tilde{D}_2 - \tilde{D}_1)\xi$ in the estimation error dynamics will prevent the error e_1 from decaying exponantionaly to zero where it represents the error source in the observation process. In fact, this term is the source of observer spillover that may cause instability in system response. Minimizing the error in the observation process is not an easy task since it influenced by the size of the reduced order model and the selected L matrix as stated by the following proposition.

Proposition (1) the estimation error for the sliding mode observer as proposed in Equation (57) will converge to a region around the origin bounded by

$$\|e_1\| = 2 \left\| (L\tilde{D}_2 - \tilde{D}_1)^T P \right\| \|\xi\| \qquad …(58)$$

Proof: Consider the following candidate Lyapunov function

$$V = e_1^T P e_1$$

where P is a positive definite matrix. The time derivative of V is

$$\dot{V} = e_1^T P^T \dot{e}_1 + \dot{e}_1^T P e_1$$
$$= e_1^T P^T \{(\tilde{A}_{11} - L\tilde{A}_{21})e_1 + (L\tilde{D}_2 - \tilde{D}_1)\xi\} + \{e_1^T(\tilde{A}_{11} - L\tilde{A}_{21})^T + \xi^T(L\tilde{D}_2 - \tilde{D}_1)^T\}P e_1$$
$$= e_1^T\{P^T(\tilde{A}_{11} - L\tilde{A}_{21}) + (\tilde{A}_{11} - L\tilde{A}_{21})^T P\}e_1 + 2\xi^T(L\tilde{D}_2 - \tilde{D}_1)^T P e_1$$
$$= -e_1^T e_1 + 2\xi^T(L\tilde{D}_2 - \tilde{D}_1)^T P e_1$$
$$\leq -e_1^T e_1 + 2\left\|\xi^T(L\tilde{D}_2 - \tilde{D}_1)^T P e_1\right\|$$
$$\leq -e_1^T e_1 + 2\|\xi\| \left\|(L\tilde{D}_2 - \tilde{D}_1)^T P\right\| \|e_1\|$$
$$= -\|e_1\|^2 + 2\|\xi\| \left\|(L\tilde{D}_2 - \tilde{D}_1)^T P\right\| \|e_1\|$$
$$= -\left\{\|e_1\| - 2\|\xi\| \left\|(L\tilde{D}_2 - \tilde{D}_1)^T P\right\|\right\} \|e_1\|$$

where $P^T(\tilde{A}_{11} - L\tilde{A}_{21}) + (\tilde{A}_{11} - L\tilde{A}_{21})^T P = -I$ is the Lyapunov equation. From the inequality above the condition $\dot{V} \leq 0$ is satisfied in the compact set defined by

$$\|e_1\| > 2 \left\|(L\tilde{D}_2 - \tilde{D}_1)^T P\right\| \|\xi\|$$

which means that the steady stat error is bounded by

$$\|e_1\| = 2 \left\|(L\tilde{D}_2 - \tilde{D}_1)^T P\right\| \|\xi\|$$

Where

$$\left\|(L\tilde{D}_2 - \tilde{D}_1)^T P\right\| = \left[\lambda_{max}\left(P^T(L\tilde{D}_2 - \tilde{D}_1)(L\tilde{D}_2 - \tilde{D}_1)^T P\right)\right]^{1/2}.$$

Remark (1): in order to minimize the state estimation error we must select the L matrix such that the norm $\left\|(L\tilde{D}_2 - \tilde{D}_1)^T P\right\|$ is minimal and, in the same time, the matrix $(\tilde{A}_{11} - L\tilde{A}_{21})$ is Hurwitz as mentioned above. This task cannot easily be handled by try and error but we try in this work to select a suitable L such that we get an appropriate estimation accuracy.

6. Simulation Results and Discussion

The simulation results for a cantilever beam, which is subjected to an initial tip deflection, are presented in this section where the MATLAB 14 software is used to simulate the cantilever beam system. The physical and geometrical specifications for the beam are given in Table (1).

Three steps are performed in the present work toward designing an active vibration control to the cantilever beam. In the first step, the natural frequencies for derived mathematical model of the beam Equation (30) are calculated and compared with the natural frequencies obtained from the ANSYS program. The results are presented in Table (2) which show a good agreement. This proves that the derived model represents the system dynamics at least with respect to the dominant natural frequencies.

Also the balance realization and order reduction process for the system model had been performed to reduce its states from twenty-four states to three states, without affecting its dominant mode. This is demonstrated in Figure (2) in the Bode plot.

Table 1,
Physical and geometrical specification for the flexible cantilever beam and the piezoelectric.

Physical Specification	Cantilever Beam	Piezoelectric
Length	L=276 mm	l_a =46 mm
Width	b =33 mm	b= 33 mm
Thickness	t_b =1 mm	t_a = 0.762 mm
Young modulus	E_b =193.06 Gpa	E_p = 68 Gpa
Density	ρ_b =8030 Kg/m^3	ρ_p = 7700 Kg/m^3
Damping coefficients	α = 0.8 & β = 6.8E-5	

Table 2.
Natural frequency results of the system

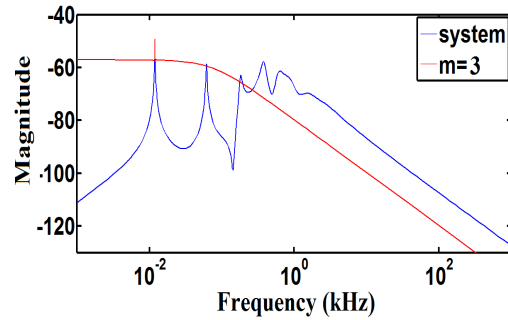| Natural Frequency	MATLAB (Hz)	ANSYS (Hz)	%Error
f_1	11.878	11.421	3.847
f_2	61.376	61.148	0.371
f_3	181.06	180.1	0.530

Fig. 2. Bode plot.

In the second step, the sliding mode observer is designed to the reduced order model. The dimension of the RM for the SMO is selected in this work equal to six while the LQR control will use only three of them. The idea behind this step is that the estimation error is decreased by using larger dimension to the reduced order model than that used in the control law.

The estimated output using the SMO states ($y = C_r x_r$, x_r is the estimated six states) is compared with actual output in Figure (3). Due to the discontinuous term injected in the SMO (v in Equation (53) with $\eta = 130000$)), the estimated output is chatters around the actual piezoelectric output. This is more clarified in Figure (4) where the error between the actual output and the estimated output Equations (46) & (51)) is plotted. The chattering effect can be removed by replacing the *signum* function Equation (54) with a continuous approximate function (the arc tan function). The *signum* function is replaced by;

$$sgn(e_y) \approx \frac{2}{\pi} * \tan^{-1}(n * e_y), \ \ n = 0.1$$

Replacing $sgn(e_y)$ by the approximation given above will prevent chattering and give smooth values for the estimated states shown in Figures (5 to 6).

By using only three of the estimated states, the designed control law based on the LQR approach is applied to the cantilever beam dynamic and the system is simulated for 15 mm initial tip displacement. The system eigenvalues after using the proposed LQR control are found in Table (3). Table (4) shows that by using reduced model of dimension three, four or six that can be selected according to the singular values, the control LQR change the value of the minimum absolute eigenvalue to the same value. So the best choice of the reduce model dimension is three.
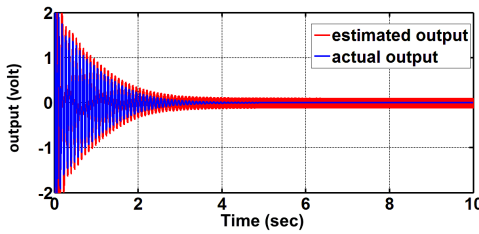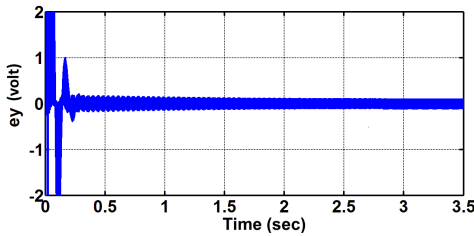
Fig. 3. The actual and the SMO sensor output.

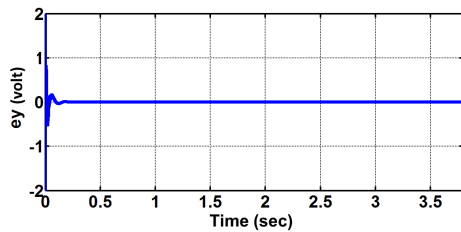**Fig. 4. The error between the actual and the estimated sensor output.**

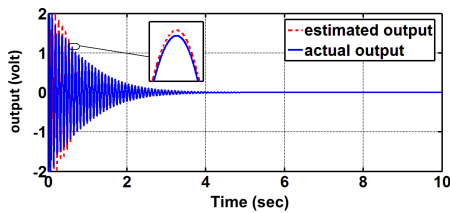**Fig. 5. The error between the actual and the estimated sensor output (with removing chattering).**

Fig. 6. The actual piezoelectric sensor output and the SMO output (with removing chattering).

Table 3,
Open and closed loop system eigenvalues.

System Eigenvalues (open loop)	New System Eigenvalues (closed loop)
-0.58936 + 74.626i	-1.5686 + 74.863i
-0.58936 - 74.626i	-1.5686 - 74.863i

The first set of numerical simulation to the control system and the SMO uses a 0.00001 second as a period of integration and with the

approximate *signum* function in the observer design as defined above. In Figure (7) the controlled tip displacement with the actual system output is compared, the ability of the controller in stabilizing the tip displacement is clarified in this figure where it required about 3 second only. In addition, the control input voltage to the piezoelectric element is plotted in Figure (8), where, as can be seen, the control input is saturated to the maximum value 200V which is the maximum design value to the piezoelectric voltage.

Table 4,
Open and closed loop minimum absolute eigenvalues.

Reduced Model	Q	R^O (Open loop)	R^C (Closed Loop)	Max Control Input Voltage
3	20* [50 50 1]		1.5686	320
4	20* [50 50 1 1]	0.5893	1.2979	340
6	20* [50 50 1 1 1]		1.3073	350

In order to approach the real situation, the time period for the observer is taken equal to 0.0001 second (i.e., the change in the estimated six states happened after each 0.0001 second), while 0.0025 second is the chosen time period where the control input changes. Consequently, the second set of numerical simulation is based on these time numerical values for both; the observer simulation period of time and for the time period required for the control input voltage to change while the time period for the control system simulation is still equal to 0.0001 second. Figure (9) plots the actual output and the estimated output with time. The effectiveness of the SMO can be detected from this figure where the idea is to force the estimated output to follow the actual one in a short time. After that, the estimated states will be used in the control law Equation (42) which will attenuate the beam vibration. The tip displacement of the open and closed loop are plotted with time in Figure (10), additionally, the control input voltage is shown in Figure (11), where, as can be seen, the vibration suppression ability is nearly the same as in the first set of simulation. This enhance the applicability of the proposed controller.
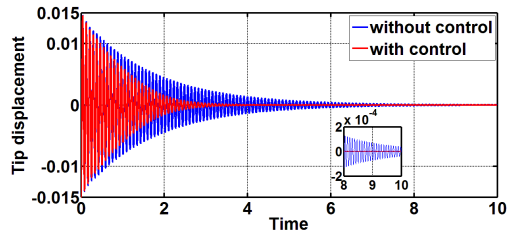
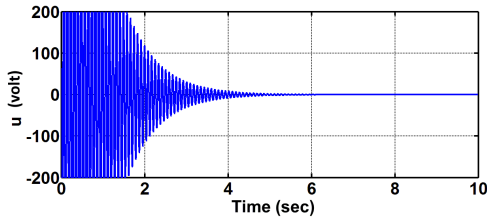**Fig. 7. Tip Displacement for open and closed loop control system.**

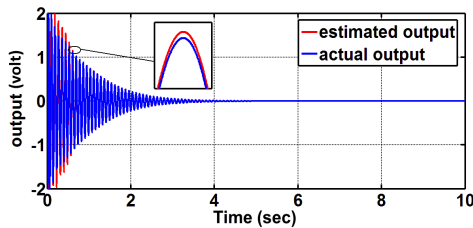**Fig. 8. The control input voltage to the piezoelectric actuator.**
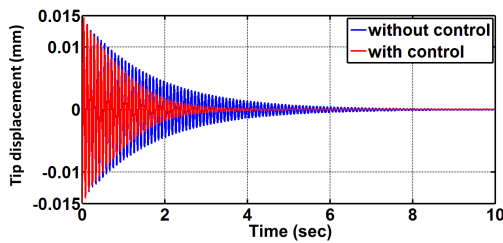

Fig. 9. The actual and the SMO sensor output.

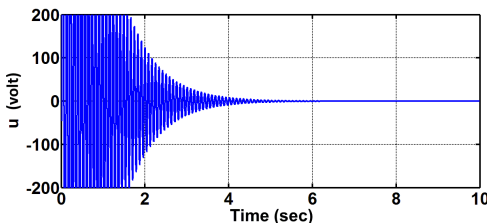**Fig. 10. Tip Displacement for open and closed loop control system.**

Fig. 11.   The control input voltage to the piezoelectric actuator.

7.   Experimental Setup and Results

The beam used in the current analysis was a stainless steel of length 276 mm, width 33 mm, and thickness 1 mm. Two piezoelectric (PZT) patches (type QP20W), of dimensions 46×33 mm and thickness 0.762 mm, were used as sensor and actuator, as depicted in Figure (1). The parameters of the flexible beam and PZT patches are given in Table (1).

The control objective is to show the effectiveness of the designed LQR controller, via the sliding mode observer, to suppress the vibration of the smart cantilever beam by means of piezoelectric elements. To achieve this control objective an experiment is set up. The experimental set up is depicted in Figure (12), which consists of a stainless beam, two PZT patches (bonded on two sides of the beam at the location indicated), accelerometer (ADXL335), two data acquisition systems (NI-PCI 6036 and NI-USB 6259), high voltage power amplifier (Trek- 601B-3), and a PC to control the system via LabVIEW program.

The beam is initially excited by 15mm tip displacement, as the beam vibrate, the stress induced in the PZT patches will generate voltages proportional to these stresses, in this case one PZT patches is working as a sensor. As the voltage signal sent to the data acquisition, type NI-6036E, the LabVIEW program, designed for this purpose using sliding mode observer, will use these signals to observe the states of the system and then fed-back to the controller. The control signals are sent to the data acquisition and then to high voltage power amplifier, type Trek-601B-3 to apply this action to the other PZT element, in this case the other PZT is used as an actuator. As a result, the vibration in the beam will be suppressed. The controller system sent signals between ±5 Volt, then these signals are amplified 40 times, by power amplifier, therefore the control signals are bounded within ±200 Volt.

The tip point displacement of the beam was measured by using the accelerometer, as shown in Figure (12). The measured signals are sent to the data acquisition type NI-6259, and then to the PC computer to the control algorithm programmed in the LabVIEW software. The acceleration signals were converted to displacement by double integral, and then plotted with time.
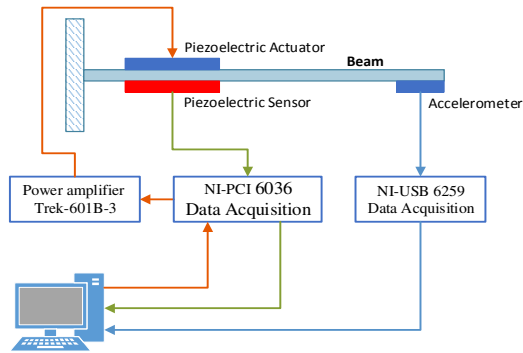
(a)
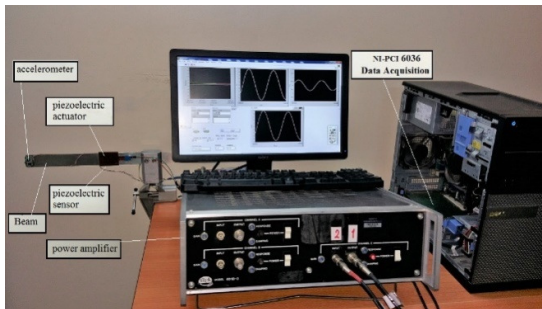
(b)

Fig. 12. Experimental set up of the flexible beam system; (a) Schematic diagram, (b) Hardware set up.

The controlled and uncontrolled tip displacement are plotted in Figure (13). It can be seen that the current control action is having the ability to suppress the tip displacement within 3 second. The PZT patch sensor output (the actual output) and the sliding mode observer output are given in Figure (14), while the voltage inputs to PZT patch actuator is shown in Figure (15). Finally, a good agreement are clear between the experimental results see Figures (13 to 15) and the results obtained from the numerical simulations Figures (9 to 11).
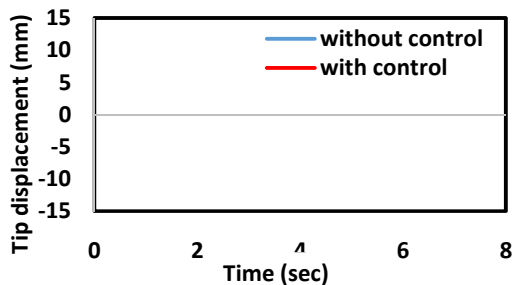

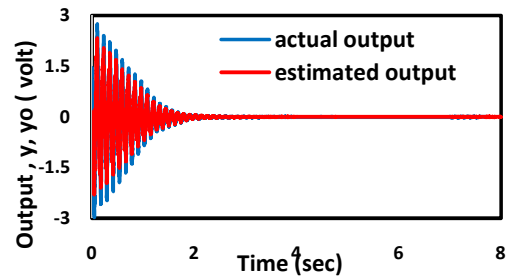**Fig. 13. Experimental tip displacement for open loop and closed loop control system.**

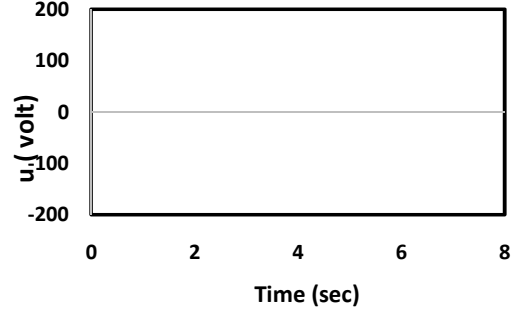**Fig. 14. The actual piezoelectric output and the SMO output.**

Fig. 15. Experimental input voltage.

8.   Conclusions

In this paper, the state space model is obtained using the finite element approach and the modal analysis resulting after appropriate modal reduction. During the theoretical calculations, the 24th order system model obtained from the finite element model is reduced to the three order using a model reduction technique based on balance realization without affecting its dominant modes.

As a basic requirement to the control design, the sliding mode observer is designed to estimates six states of the reduced model. In spite of the presence of the unknown inputs, which due to the residual model in the observer dynamics, the SMO forces the output, which is determined from the estimated states, to follow the actual output. This is taken place after approximately two seconds. After that, the reduced model states are estimated with bounded error.

To overcome the chattering problem in observer dynamics the signum function is replaced with the approximation given by the *arctan* function with appropriate parameters. As a result, the chattering is prevented and the estimated states values become more smooth.

Using the estimated states, an LQR approach was designed based on the reduced order model. The control spillover was avoided by satisfying the avoidance condition where the minimum absolute real eigenvalue is three times to that for

the matrix A Equation (30). With the proposed LQR control and the SMO, the results show that for 15 mm initial tip displacement, the piezoelectric actuator reduces the tip displacement to about 0.1 mm during 3 s.

The performance of the designed controller is examined experimentally where the results are shown very satisfactory and very close to the theoretical analysis.

Notation

A_b	Cross-section area of the beam element (mm^2).
Ap	Cross-section area of the piezoelectric element, (mm^2).
A	State matrix.
b	Width of the beam (mm).
B	Input matrix.
c	Constant which equal to $\sqrt{\frac{EI}{\rho A}}$
C	Output matrix.
d_{31}	Piezoelectric constant.
e_{31}	Piezoelectric stress/charge constant.
E_b	Young modulus of the beam (Gpa).
E_p	Young modulus of the piezoelectric (Gpa).
f_{ext}	External force (N).
f_{ctrl}	Control force (N).
F_1, F_2	Force acting at the node (N).
G_c	Signal condition device.
h	Constant vector.
$i(t)$	Sensor current.
k_b	Stiffness matrix of the beam element (N/M).
k_p	Stiffness matrix of the piezoelectric element (N/M).
l_b	Length of the beam element (mm).
L	Length of beam (mm).
M_b	Mass matrix of the beam element.
M_p	Mass matrix of the piezoelectric element.
N	Shape function.
q	Vector displacement.
	Velocity vector.
$\ddot{q}$	Acceleration vector.
R^O	Minimum absolute real eigenvalue
R^C	Minimum absolute real eigenvalue
t_a	Thickness of the actuator, (mm).
t_b	Thickness of the beam,(mm).
T	Kinetic energy ($N.M$).
u	Control input (volt).
U	Strain energy ($N.M$).
V_a	Actuator voltage (volt).
V_s	Sensor voltage (volt).
$w(x,t)$	Displacement function.
w	Degree of freedom.
α , β	Damping coefficient.
ε	Strain.
ρ_b	Density of the beam (Kg/m^3).
ρ_p	Density of the piezoelectric patch (Kg/m^3).

9. References

[1] Mehmet, I. Metin U.S.; Demet U.; and Yavuz Y.: Active Vibration Suppression of a Flexible Beam via Sliding Mode, IEEE Conference on Decision and Control, 44, 1240-1245 (2005).

[2] Junfeng, H. and Dachang, Z.: Vibration Control of Smart Structure Using Sliding Mode Control with Observer, Journal Of Computers, 7 (2), 411-418 (2012).

[3] Bandyopadhyay, B. and Mehta, A.: Vibration Control of Smart Structure Using Second Order Sliding Mode Control, IEEE Conference on Control Applications, 6 (1), 1691-1696 (2005).

[4] Kumar, S.; Srivastava, R. and Srivastava, R.K.: Active Vibration Control of Smart Piezo Cantilever Beam Using Pid Controller, International Journal of Research in Engineering and Technology, 3 (1), 392-399 (2014).

[5] Sachs, G.: Intrinsic Dynamic Analysis and Control Design, USA (2004).

[6] Inman, D.J.: Vibration with Control, USA: John Wiley & Sons Ltd (2006).

[7] Moor, B.C.: Principal Component Analysis in Linear Systems: Controllability, Observability, and Model Reduction, Transactions on Automatic Control, 26(1), 17-32 (1981).

[8] Zhou K.; Salomon, G. and Wu, E.: Balanced Realization and Model Reduction for Unstable Systems, International Journal of Robust and Nonlinear Control, 9, 183-198 (1999).

[9] Meirovitch, L.: Dynamics and Control of Structures, USA: John Wiley & Sons (1990).

[10] Dong, X.; Peng, Z.; Zhang, W.; Hua, H. and Meng, G.: Research on Spillover Effects for Vibration Control of Piezoelectric Smart Structures by ANSYS, Mathematical Problems in Engineering, 2014, 1-8 (2014).

[11] Dorf, R.C.: Optimal Control System, New York: CRC Press LLC (2003).

[12] Oveisi, A. and Nestorović, T.: Robust Mixed H2/H∞ Active Vibration Controller in Attenuation of Smart Beam, Mechanical Engineering , 12(3), 235-249 (2014).

[13] Utkin, V.: Sliding Mode Control in Electro-Mechanical Systems, New York: Taylor & Francis Group (2009).

[14] Ko, H.; Lee, K. and Kim, H.: An Intelligent Based LQR Controller Design to Power System Stabilization, Electric Power Systems Research, 71, 1-9 (2004).

[15] Alavinasab, A. and Moharrami, H.: Active Control of Structures Using Energy-Based LQR Method, Computer-Aided Civil and Infrastructure Engineering, 21, 605-611 (2006).

[16] Ericsson, A.J.; Beter, M. and Guangqlan, X.: The Optimal LQR Digital Control of a Free-Free Orbiting Platform, Acta Astronautica, 29(2), 69-81 (1993).

[17] Aldemir, U.; Bakioglu, M. and Akhiev, S.S.: Optimal Control of Linear Buildings under Seismic Excitations, Earthquake Engineering and Structural Dynamics, 30, 835-851 (2001).

[18] Luenberger, D.G.: An Introduction to Observers, IEEE Transactions on Mjtomatic Control, 16 (6), 596-602 (1971).

[19] Edwards, C.; Spurgeon, S.K. and Patton, R.J.: Sliding Mode Observers for Fault Detection and Isolation, Automatica, 36, 541-553 (2000).

[20] Liapunov, A.: Stability of Motion, New York: Academic press (1966).

[21] Karanjit Kalsi; Jianming.L.; Steven H.; and Zak, S.H.: Sliding-mode Observers for Systems with Unknown Inputs: A high-gain approach," Automatica, 46 (2010).

[22] Hashimoto H; Utkin, V.I.; Xu, J.X., Hiroyuki S. and Fumio H.: Vss Observer for Linear Time Varying System, Proceedings of the Industrial Electronics, (1990).

[23] Walcot, B.L. and Zak, S.H.: Combined Observer- Controller Synthesis for Uncertain Dynamical Systems with Applications, IEEE Transactions On Systems, 18 (1) (1988).

[24] Decarlo, R.A. ; Zak, S.H.; and Matthews G. P.: Variable Structure Control of Nonlinear Multivariable Systems: a Tutorial, IEEE, 76 (3), 212-232 (1988).

[25] Slotion, J.J.E.; Hedrick, J. K. and Misawa, E. A.: On Sliding Observers for Nonlinear System, Dynamic of System Mechanical and Control, 109, 245-252 (1987).

[26] Singiresu S. Rao: Vibration of Continuous System,USA: John Wiley & Sons, Inc. (2007).

[27] Chhabra, D.; Narwal, K. and singh, P.: Design and Analysis of Piezoelectric Smart Beam for Active Vibration Control, International Journal of Advancements in Research & Technology, 1 (1), (2012).

[28] Manjunath, T.C. and Bandyopadhyay, B. Controller Design for Euler-Bernoulli Smart Smart Structures Using Robust Decentralized FOS via Reduced Order Modeling, International Journal of Electrical and Computer Engineering 1:6 (2006).

[29] Shibly, A.; Mohsin N. and Imad A. Vibration Suppression Control for a Flexible Beam with Sliding Mode Observer, Al-Nahrain University, College of Engineering Journal (NUCEJ) Vol.19, No.2, pp.327 – 341 (2016).

[30] Bandyopadhyay, B.; Manjunath, T.C. and Umapathy, M.: Modeling, Control and Implementation of Smart Structures, Germany: Verlag Berlin Heidelberg, (2007).

[31] Deepak, C.; Pankaj, C. and Gian B. Design and Analysis of Smart Structures for Active Vibration Control using Piezo Crystal, International Journal of Engineering and TechnologyVolume 1 No. 3, (2011).

[32] Jayant, S. and Inderjit, C. Fundamental Understanding of Piezoelectric Strain Sensors, Journal of intelligent material systems And structures, Vol. 11, (2000).

[33] Jalili, N.: Piezoelectric-Based Vibration Control, USA: Springer Science+Business Media, LLC, (2010).

[34] Manjunath, T.C. and Bandyopadhyay, B. Controller Design for Euler-Bernoulli Smart Smart Structures Using Robust Decentralized POS via Reduced Order, International Journal of Mechanical, Vol:1, No:6, (2007).

[35] Balamurugan, V. and Narayanan, S.: Active Vibration Control of Piezolaminated Smart Beams, (2000).

[36] Clough, R. W. and Penzien, J.: Dynamics of Structures, Computers & Structures, Inc. (2003).

[37] Manjunath, T.C. and Bandyopadhyay, B. Smart Control of Cantilever Structures Using Output Feedback, I.J. of Simulation Vol. 7 (2007).

[38] Williams, R.L. and Lawrence, D.A.: Linear State-Space Control Systems, USA: John Wiley & Sons, Inc. (2007).

[39] Ralf, P.; Martine O. and Bernard H. Balanced Realization of Lossless Systems:

[40] Schur Parameters, Canonical Forms and Application, 6-8, (2009).

[41] Moor, J.B.: Optimal Control Linear Qardatic Methods, USA: Prentice- Hall (1989).

تخميد الاهتزازات للعتبة الكابولية الذكية مع المخمن المنزلق الشكل باستخدام اثنين من المواد الكهروضغطية

شبلي احمد السامرائي*   **محسن نوري حمزة*****

عماد عبد الحسين عبد الصاحب***

*قسم هندسة السيطرة والنظم / الجامعة التكنولوجية

، ** قسم الهندسة الميكانيكية / الجامعة التكنولوجية

* البريد الالكتروني: 60132@uotechnology.edu.iq

** البريد الالكتروني: dr.mohsin@uotechnology.edu.iq

*** البريد الالكتروني: emad099@yahoo.com

الخلاصة

يقدم هذا البحث تصميما لمسيطر إخماد الاهتزاز في عارضة ناتئة باستخدام اثنين من المواد الكهروضغطية. تم لصق المواد الكهروضغطية على سطح العارضة لتعمل مشغلا ميكانيكيا (actuator) ومتحسسا. هناك مصدران من عدم الاستقرار في العتبة، وهما تأثير تداعيات المخمن وتأثير تداعيات السيطرة غير المباشرة، حيث تم اخذ هذين المصدرين بنظر الاعتبار في التصميم الحالي لنظام السيطرة على أساس انموذج مخفض من النظام الأصلي. لتصميم نظام تحكم والذي من شأنه تخفيف الاهتزاز، تم استخدام طريقة (Balance realization) لاختيار انموذج مخفّض حيث يكون هذا النموذج أكثر قابلية على السيطرة والتخمين. تم اختيار ثلاثة متغيرات للنموذج المخفض عن النظام الأصلي. ان نظام المخمن المنزلق، والذي يستند على المسيطر المكافئ، يهدف إلى تقدير ستة متغيرات حيث إن الخطأ في التخميد محدد كما تم إثباته. باستخدام تخمين المتغيرات عن طريق المخمن المنزلق، تم تصميم وحدة تحكم LQR الأمثل من شأنها أن تخفف من اهتزاز العتبة الذكية وباستخدام العنصر الكهروضغطي. وللتغلب على مشكلة تأثير السيطرة غير المباشرة، تم اشتقاق شرط تحقيق الاستقرارية والذي يضمن استقرار المسيطر للتصميم المقترح والذي سيقلل الاهتزاز في العتبة. باستخدام المحاكاة العددية تم اختبار قدرة نظام السيطرة المقترح لتقليل الاهتزاز وتخميده. كما تم ازاحة طرف العتبة ١٥ مم، حيث وجد بان المشغل الميكانيكي للمادة الكهروضغطية قادر على تقليل الازاحة إلى حوالي ١.٠ ملم بعد ٤ ثانية، في حين أن قيمتها ١.٥ ملم في الحالة الحرة. اظهرت النتائج العملية على العتبة الذكية الأداء المتميز لقانون السيطرة والمسيطر منزلق الشكل المقترح.